Environmental Science: Atmospheres

ROYAL SOCIETY OF CHEMISTRY

PAPER

View Article Online
View Journal

Cite this: DOI: 10.1039/d5ea00175g

Effects of an electrostatic precipitator on particle mass, composition, and number size distributions in residential wood combustion emissions

Narayan Babu Dhital, *[ab] Juho Louhisalmi,[a] Henna Rinta-Kiikka,[a] Sampsa Väätäinen,[a] Jani Leskinen,[a] Olli Sippula[ac] and Jarkko Tissari[a]

Residential wood combustion (RWC) is an increasingly dominant source of particulate matter (PM) pollution in Europe. Electrostatic precipitators (ESPs) are a promising technology for controlling particle mass emissions from RWC appliances, but their influence on particle number concentrations (PNC) is highly variable, as they may occasionally increase PNC. In this study, we evaluated the effect of an ESP on PM_1, black carbon (BC), elemental carbon (EC), organic carbon (OC), and particle number size distributions in emissions from wood-fueled stoves commonly used in Finland, under conditions spanning a wide range of upstream emission loads. Experiments were conducted in a state-of-the-art small-scale combustion simulation and measurement facility. The emission reduction efficiencies of the ESP were 75.7% ± 4.7% for PM_1, 83.2% ± 14.2% for EC, and 70.1% ± 12.6% for OC. The operation of ESP not only reduced PM_1 concentrations but also influenced particle composition and optical properties with its differential collection efficiencies for EC and OC. Moreover, it reduced PNC within the size range of 0.13–2.5 μm, but nucleation-mode PNC occasionally increased, suggesting possible new particle formation. Additionally, the combustion conditions that showed negative efficiencies for PNC had higher upstream organic gaseous carbon concentrations and higher OC : EC ratios compared to those with positive efficiencies, suggesting that organics-rich flue gas may contribute to increased PNC when ESPs are used. These findings highlight the importance of controlling organic emissions to improve the overall emission reduction performance of ESPs.

Received 24th December 2025
Accepted 20th May 2026

DOI: 10.1039/d5ea00175g

rsc.li/esatmospheres

Environmental significance

This study evaluated the performance of an electrostatic precipitator as a secondary emission control technology for residential wood combustion appliances. It demonstrated a significant reduction in particle mass emissions. However, it showed a highly variable impact on particle number emissions, with possible new particle formation occurring within the electrostatic precipitator, highlighting the complexity of residential wood combustion emission control. Optimizing primary and secondary control measures for both particle mass and number emissions is a crucial step toward developing comprehensive mitigation strategies.

1 Introduction

Bioenergy constitutes a major share of the European Union's (EU) energy landscape.[1] In 2023, renewable energy accounted for nearly one-fourth of the EU's gross final energy consumption, with bioenergy accounting for approximately half of that share.[2] Although biomass fuels are considered a renewable and sustainable energy source with potential carbon neutrality compared to fossil fuels,[3] they are an important source of short-lived climate forcers[4] and a significant contributor to air pollution.[5,6] As emission standards become increasingly stringent for historically dominant sectors like transport, emissions from those sectors have declined.[7] Meanwhile, the relative contribution of residential wood combustion (RWC) emissions has increased across the EU.

In Finland, wood combustion accounts for approximately one-fifth of total household energy consumption.[8] RWC constitutes a key source of emissions of particulate pollutants, especially black carbon (BC) and fine particulate matter ($PM_{2.5}$), in the country.[4] The contribution of the residential stationary combustion sector to Finland's total $PM_{2.5}$ emissions increased sharply from 16.8% in 1990 to 56.1% in 2023.[7] This trend highlights the growing importance of addressing RWC emissions as part of broader efforts to reduce air pollution in Finland further.

[a]Department of Environmental and Biological Sciences, University of Eastern Finland, 70210 Kuopio, Finland. E-mail: narayan.dhital@uef.fi; nbdhital@gmail.com
[b]Department Environmental Science, Patan Multiple Campus, Tribhuvan University, 44700 Lalitpur, Nepal
[c]Department of Chemistry and Sustainable Technology, University of Eastern Finland, 80101 Joensuu, Finland

The implementation of EU Regulation (2015/1185/EU) under the Ecodesign Directive (2009/125/EC) introduced stricter performance criteria and emission thresholds for particulate matter (PM), organic gaseous carbon, carbon monoxide (CO), and nitrogen oxides (NO_x) for solid fuel local space heaters beginning in 2022. These progressively tightening standards and thresholds require manufacturers to significantly reduce emissions in new RWC appliances, which can be achieved through a combination of primary measures, such as air staging and automatic combustion control, and secondary measures using post-combustion technologies, such as catalysts and particle filters. Although optimizing combustion can lower emissions, it may entail tradeoffs between different pollutants and energy efficiency.[9] For example, in a study on sauna stove emissions, the use of secondary air supply reduced both particulate and gaseous emissions but decreased thermal efficiency.[9] Moreover, heat exchanger fans and exhaust fans can have competing effects on stove efficiencies and emissions.[10] Even with modern appliances, user behavior and operational practices often result in higher emissions than those anticipated under optimal operating conditions.[11,12] Moreover, the new limits under the Ecodesign Directive are unlikely to substantially reduce particulate emissions from RWC in Finland, primarily because they do not cover sauna stoves and older, existing appliances.[11] To achieve significant emission reductions in the RWC sector, it is essential to control emissions from old high-emitting appliances, for example, by replacing such units with low-emission models or retrofitting them with secondary controls, such as particle filters.

Electrostatic precipitators (ESP) are particulate emission control devices that function by using corona discharge electrodes for electrically charging particles and separating them from the gas stream in a strong electric field, subsequently collecting them on a collection electrode. While field charging is the dominant mechanism for larger particles (>1 μm), diffusion charging, which occurs through random collisions of unipolar ions with particles due to Brownian motion, dominates for ultrafine particles[13] and is an important charging mechanism in small-scale ESPs. ESPs employ several different designs, such as plate-wire precipitators, flat-plate precipitators, filter-bed precipitators, two-stage precipitators with separate units for charging and precipitation, tubular ESPs, and shielded corona chargers.[14,15] The plate-wire design is common in large-scale industrial applications.[16] High-resistivity particles, which increase ESP susceptibility to back corona, can be effectively controlled by the flat-plate precipitators.[16] Shielded corona chargers have been reported to be suitable for residential-scale biomass-fueled boilers due to their small space requirement and simple design.[15] Additionally, high-temperature electric soot collectors are specialized filters that use electric fields to capture flame-ionized fine particles and oxidize them within the combustion chamber.[17] Tubular ESPs, which are well suited for wet or sticky emissions,[16] are a common type used in wood stoves. Although ESPs are a mature technology for industrial emission control, their use in RWC appliances is challenging due to highly variable emission loads and flue gas flow rates, as well as high flue-gas temperatures. On the positive side, ESPs offer the advantage of low pressure drop[18] and high particle collection efficiency,[19,20] making them suitable for natural-draft appliances.

PM collection efficiencies of ESPs have been reported to range from 99.8% in biomass power plants,[21] 93% (total suspended particulate) and 98% (PM_1) in high-emitting wood combustion appliances[22] to 71% (PM_1) in a modern stove.[23] However, efficiencies as low as 29% (PM_{10}) have also been reported.[24] This variation reflects the differences in the ESP design and operational parameters,[25,26] as well as external factors associated with the emission source, such as flue gas temperature and velocity, emission load, particle size distribution, and chemical composition. Efficiency generally decreases with increasing flue gas temperatures and velocities.[27,28] This deterioration in efficiency is partly due to a reduced operating voltage and air density at higher temperatures.[29] ESP efficiency is highly variable across combustion phases due to changes in flue gas temperatures and velocities, as well as particle concentrations, electrical conductivities, and size distributions between phases.[22,23,27] In a study on a modern wood stove, ESP efficiency progressively decreased in a sequence of combustion batches, plausibly due to a reduction in ESP power during the later batches.[23] Furthermore, ESPs may also influence gaseous emissions such as NO_x and hydrocarbons.[30] It has been suggested that NO_x chemistry within ESPs might lead to the formation of nitric acid particles and may also promote secondary aerosol formation through ion-induced nucleation, potentially affecting the overall PM collection efficiency.[31]

Although ESPs generally have high particle mass collection efficiency, albeit with notable variability, their effect on particle number concentrations (PNC) and number size distributions is even more variable across the literature.[23,27] For instance, Cornette *et al.* reported accumulation-mode particle number collection efficiency of a tubular ESP in a 240 kW continuously-fed wood chip boiler ranging from approximately 84% to 92%.[32] Likewise, an ESP reduced PNC in emissions from a 15 kW automated wood pellet boiler from 48% to 64%.[33] In contrast, a study with a batch-operated wood stove fitted with a tube-type ESP reported new particle formation within the ESP, characterized by elevated PNC for particles smaller than 30 nm, thus exhibiting negative PNC reduction efficiency within this size bin.[23] Corona discharge chemistry within ESPs produces ozone,[34–36] which can oxidize organics and potentially contribute to new particle formation. A study found higher proportions of oxygenated compounds in particles with an ESP than without it, likely due to a low particle-to-oxidant ratio and ozone-induced aging of flue gas.[37] These findings indicate that PNC reduction efficiency of ESPs is highly dependent on operating conditions and can sometimes even lead to unintended new particle formation.

Given the limited research on potential new particle formation within ESPs and on how ESPs affect PNC and number size distributions in RWC emissions, this study provides a comprehensive evaluation of ESP performance in a traditional sauna stove and a modern local space heater. We investigated the effects of ESP operation across a range of emission loads by integrating measurements of PM_1, BC, elemental carbon (EC),

organic carbon (OC), PNC, particle number size distributions, and various gaseous emissions from the selected RWC appliances.

2 Materials and methods

2.1 Experimental design

The experiments were designed to evaluate ESP performance on RWC appliances across various operating conditions and emission loads. The two stoves tested were a traditional wood sauna stove (SS) and a modern non-heat-retaining wood stove (MS) (Aduro 9.3, Aduro A/S, Aarhus, Denmark). SS and MS had nominal powers of 20 and 6 kW, respectively. The SS firebox volume was approximately 40 000 cm^3. The MS firebox had a width of 48 cm, a depth of 37 cm, and a height of 43 cm. The photographs of the test stoves are provided in the SI (Fig. S1).

Typically, sauna stoves contain stones packed inside a stone cage above the firebox. These stones act as a heat-storage medium. Water is poured over the hot stones to produce steam, which then heats the sauna room. The modern wood stove used in this study was a typical small-scale space heater and did not include any heat-storage structures. Both stoves had a metal grate on the bottom of the firebox that provided the primary air supply. Additionally, a heated secondary air supply is provided into the flame zone. Detailed information on various combustion air pathways, including the SA flow, in SS can be found in a previous study.[9] We retrofitted both stoves with a commercial tube-type ESP (OekoTube-Inside, Switzerland). The ESP is designed to be integrated into the chimney and can be used with various types of small-scale wood, pellets, and coal-fueled stoves (<40 kW). The ESP operation is automatically controlled based on the temperature signal from a built-in temperature sensor that activates the ESP when a threshold temperature is exceeded. It also features an automated voltage and power control system that optimizes the operating conditions to maximize power while minimizing sparkover occurrences. If sparkovers occur, the system automatically reduces the power to maintain stable operation.[22]

To span a wide range of PM_1 emission loads, various combinations of stove types and operating conditions were used. Operation of SS without secondary air (SA) supply, imitating the operation of old-model stoves that lack SA supply in their designs, was used to represent a high-emission load scenario. Similarly, SS with SA supply was used as a medium-emission load scenario, whereas MS operation represented a low-emission load scenario. Additionally, the SS operation involved ignition (batch 1) and hot-stove combustion (batch 2), with batch 2 having notably higher emission levels than batch 1, and hence these two batches were treated as different experimental conditions. In SS tests, batch 1 had an average fuel load of 2993 ± 29 g (mean ± standard deviation, SD), and batch 2 had a fuel load of 3014 ± 14 g. Moreover, the operation of MS consisted of a sequence of seven batches followed by char combustion, with a fuel load of 1851 ± 1.5 g in the ignition batch and 1999 ± 7.6 g in the successive batches.

Altogether, there were the following five experimental conditions: SS without SA (batch 1), SS without SA (batch 2), SS with SA (batch 1), SS with SA (batch 2), and MS. Furthermore, emissions were tested under each of these five conditions without ESP (control, C) and with ESP (treatment, T). All SS tests had three replicates, whereas MS control and MS treatment had 11 and 10 replicates, respectively, making a total of 45 test batches (Table 1). In all cases without ESP, PM_1 was higher than the current Ecodesign limits in Europe.

To ensure comparable conditions between the control and treatment groups, fuel quality and loads were kept similar within each pair. Birch wood logs (approximately 30 cm in length and 15% moisture on a wet basis) were used as fuel across all experiments. Fuel moisture was determined using the oven-dry method (SFS-EN ISO 18134-2:2015). In both stove types, wood logs were initially arranged in a criss–cross pattern and ignited from the top of the stack. For subsequent fuel batches, wood logs were added lengthwise as a bundle on top of the existing ember bed. For SS, the control and treatment group fuel loads were 3009 ± 12.1 g and 2998 ± 32.2 g, respectively. For MS tests, the corresponding fuel loads were 1973 ± 60.7 g (control) and 1983 ± 47.0 g (treatment). For both stove types, the

Table 1 Test conditions and sample size

Appliance[a]	Test description[a]	Test code[a]	Experimental group[a]	Sample size (n)
SS	SS without SA (baseline), batch 1	SS_BL (B1)	C	3
	SS without SA (baseline), batch 2	SS_BL (B2)	C	3
	SS with ESP but without SA, batch 1	SS_ESP (B1)	T	3
	SS with ESP but without SA, batch 2	SS_ESP (B2)	T	3
	SS with SA, batch 1	SS_SA (B1)	C	3
	SS with SA, batch 2	SS_SA (B2)	C	3
	SS with SA and ESP, batch 1	SS_SA + ESP (B1)	T	3
	SS with SA and ESP, batch 2	SS_SA + ESP (B2)	T	3
MS	MS (baseline)	MS_BL	C	11
	MS with ESP	MS_ESP	T	10
SS and MS	—	—	C + T	45

[a] SS = traditional wood sauna stove, MS = modern wood stove, BL = baseline, SA = secondary air supply, ESP = electrostatic precipitator, C = control, T = treatment, B1 = batch 1, B2 = batch 2.

difference in fuel mass per batch between the control and treatment tests is less than 0.6% of the average fuel mass per batch, which is negligible to have any notable effect on observed differences in emissions. The mean duration of each batch across all experimental conditions was 36 ± 5.1 min.

2.2 Sampling and measurement system

Combustion experiments were conducted in the small-scale combustion simulator (SIMO) at the University of Eastern Finland.[38] The SIMO facility comprises a sauna room and a measurement container, both housed in separate marine containers. RWC appliances were operated in the sauna room, and flue gas was channeled to the measurement container with a stainless-steel chimney fitted with a fan to generate the necessary draft. The measurement container is a state-of-the-art facility designed for comprehensive sampling and analysis of gaseous and particulate pollutants. Various components of the sampling and measurement system, including calibration and measurement ranges, are provided in the SI (Table S1).

Flue gas samples for online gas analyzers were drawn from the chimney through a heated sample line (180 °C) fitted with a ceramic filter. Total hydrocarbons (THC) were measured in the raw flue gas using a Siemens THC analyzer equipped with a flame ionization detector (FIDAMAT 6, Siemens AG, Nürnberg, Germany), while CO, NO, and CO_2 concentrations were measured in dried flue gas with Siemens gas analyzers (Ultramat 23, Siemens AG, Nürnberg, Germany). Concentrations of volatile organic compounds (VOCs) were measured using a Fourier-transform infrared analyzer (FTIR, DX4000, Gasmet Technologies Ltd., Vantaa, Finland). VOC measurements were used to calculate organic gaseous carbon (OGC) concentrations.

The particulate sampling system consisted of a heated sample line (200 °C) equipped with an upstream pre-cyclone and a downstream two-stage dilution system.[39] The dilution system included a porous tube diluter and an ejector diluter, and raw flue gas was diluted using dry, particle-free pressurized air. The dilution ratio was automatically calculated and controlled by a computer program using CO_2 concentrations in raw flue gas, dilution air, and diluted flue gas, measured by CO_2 analyzers (GMP343, Vaisala, Vantaa, Finland). Mean dilution ratios were 90 and 46 for SS and MS tests, respectively. Batch-integrated particle samples were collected downstream of a PM_1 impactor on both Teflon membrane filter (TF, 47 mm, Pall Corporation, USA) and quartz fiber filters (QF, 47 mm, Pall Corporation, USA). The filters were conditioned and then weighed using a microbalance (Mettler Toledo, MT5, Ohio, USA), both before and after sampling. The PM_1 fraction was analyzed because it represents a major fraction of particulate emissions from RWC appliances.[40] In addition, PM_1 is also a more repeatable emission metric than total PM in RWC emissions. TF was used for gravimetric PM_1 measurements, while QF was used for EC and OC analyses. The QF placed downstream of the TF provided an estimate of gaseous OC artifact, which was subtracted from the total OC to obtain particle-phase OC.[39] The EC and OC analyses were performed using a thermal-optical carbon analyzer (Sunset Laboratory Inc., Portland, USA), following the NIOSH 870 protocol.

Downstream of the dilution system, an electrical low-pressure impactor (ELPI, Dekati Inc., Kangasala, Finland) was used to measure particle mass concentration ($PM_{1,ELPI}$) and number size distribution. Moreover, an additional ejector diluter was installed for measuring PNC using a condensation particle counter (CPC 3775, TSI Inc., Minnesota, USA). Likewise, BC and absorption Ångström exponent (AAE) were measured using an aethalometer (AE33-7, Magee Scientific, Berkeley, USA). A schematic of the sampling and measurement system is presented in Fig. 1. Additional details of the SIMO facility and the sampling equipment can be found in previous publications.[39,41]

2.3 Data processing and analysis

Data from online instruments were averaged and recorded at 10 s intervals. All gaseous concentrations were standardized to normal temperature and pressure (NTP) and 13% O_2. Similarly, particulate concentrations were also standardized to NTP and 13% O_2 and corrected for dilutions using eqn (1).[41]

$$C_{\mathrm{cor},i} = C_{\mathrm{raw},i} \times \left(\frac{\mathrm{CO_{2,ST}} - \mathrm{O_{2,N}} - \mathrm{CO_{2,BG},i}}{\mathrm{CO_{2,D},i} - \mathrm{CO_{2,BG},i}}\right) \times \left(\frac{T_{\mathrm{n}} \times P_{\mathrm{s}}}{T_{\mathrm{s}} \times P_{\mathrm{n}}}\right) \quad (1)$$

In eqn (1), $C_{\mathrm{cor},i}$ is the dilution corrected concentration of a pollutant normalized to standard O_2 concentration ($O_{2,N}$, 13%) at normal temperature (T_n, 273.15 K) and pressure (P_n, 1 atm), and i represents the time step. Likewise, $C_{\mathrm{raw},i}$ is the raw concentration of the pollutant, whereas $CO_{2,ST}$, $CO_{2,BG,i}$, and $CO_{2,D,i}$ are stoichiometric CO_2 concentration in flue gas (20.2%), CO_2 concentration in dilution air, and CO_2 concentration in diluted sample, respectively. Similarly, T_s and P_s represent sample air temperature and pressure, respectively. A more detailed description of the data processing steps is provided in a previous publication.[41]

The batch-average concentrations were compared between the control and treatment groups under five different test conditions (SS without SA batch 1, SS without SA batch 2, SS with SA batch 1, SS with SA batch 2, and MS). Statistical significance, where applicable, was assessed at the 0.05 level. ESP efficiencies were calculated using average pollutant concentrations in the control and treatment groups (eqn (2)).

$$\eta_{j,k}\ (\%) = \left(1 - \frac{C_{j,k,\mathrm{T}}}{C_{j,k,\mathrm{C}}}\right) \times 100 \quad (2)$$

In eqn (2), $\eta_{j,k}$ is the ESP efficiency for the pollutant j under the k^{th} test condition, $C_{j,k,\mathrm{C}}$ is the mean control concentration of the pollutant j under the k^{th} test condition, and $C_{\mathrm{j,k,T}}$ is the mean treatment concentration of the pollutant j under the k^{th} test condition.

Additionally, fuel-mass-specific emission factors (EF_{fuel}) were calculated following the method reported by a previous study.[42] The detailed method of the calculation of emission factors has been provided in the SI (SM-1).

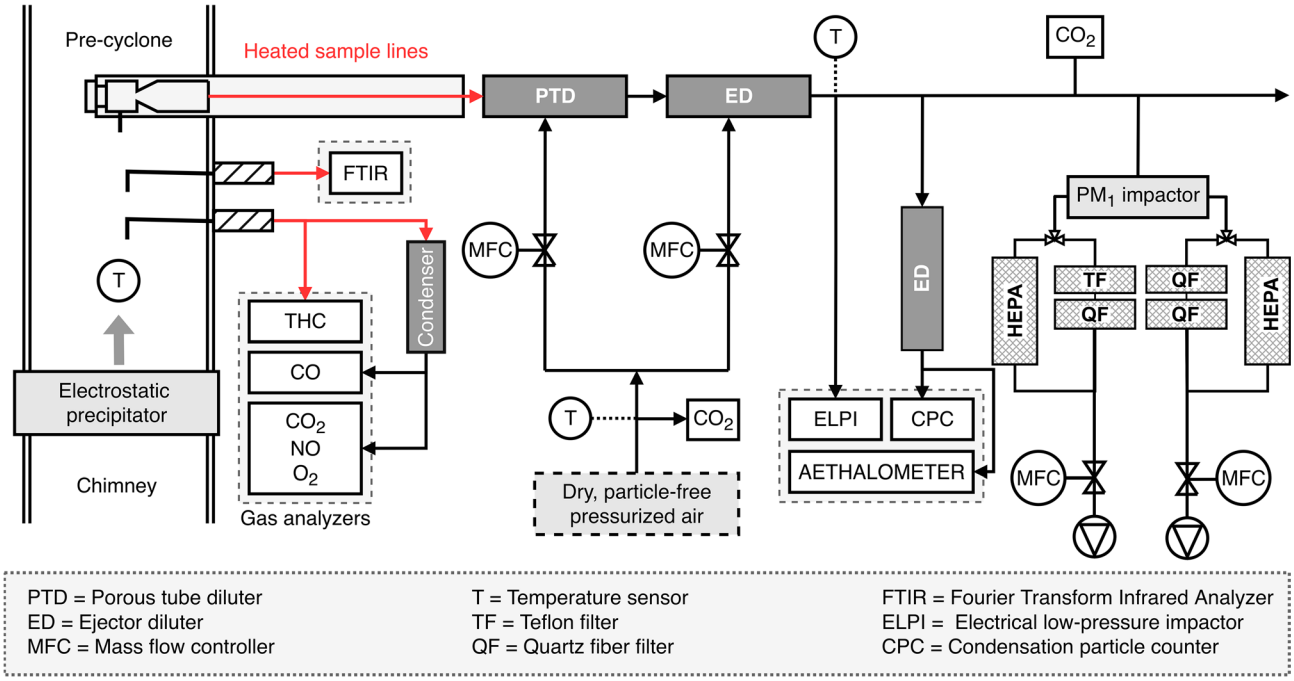

Fig. 1 Schematic of the sampling and measurement system.

2.4 Quality control and assurance

We simultaneously measured batch-integrated gravimetric PM_1, real-time $PM_{1,ELPI}$, real-time BC, and batch-integrated OC and EC. A scatter plot of gravimetric batch-average PM_1 *vs.* BC and EC (SI, Fig. S2) shows strong linear relationships. However, in a few low-emission batches, gravimetric PM_1 concentrations were slightly less than BC or EC (points above the 1 : 1 line in SI, Fig. S2a and b). However, BC concentrations agreed very well with EC concentrations (SI, Fig. S2c). Together, these results indicate measurement issues with gravimetric PM_1 in a few low-emission samples (seven out of 45 test batches), likely due to low gravimetric PM_1. We therefore corrected the raw $PM_{1,ELPI}$ using valid gravimetric PM_1 only, and used these corrected $PM_{1,ELPI}$ data in subsequent analyses of ESP collection efficiency.

3 Results and discussion

3.1 Comparison of flue gas characteristics between treatment and control groups

Of the 45 test batches, 23 were control batches, and 22 were treatment batches. A summary of flue gas properties and particulate and gaseous concentrations for both groups is presented in Fig. 2, with detailed batch-level data provided in SI (Table S2). We also calculated fuel-mass-specific emission factors. However, because comparisons between the treatment and control groups lead to the same conclusions, whether based on standardized concentrations or emission factors, our main discussion focuses on standardized concentrations, while detailed batch-level emission factors are provided in the SI (Table S3).

Differences between the control and treatment groups were assessed using a *t*-test when data were normally distributed, and a Mann–Whitney *U* test otherwise. To minimize the influence of confounding factors, each control–treatment pair was tested under identical combustion conditions (*e.g.*, fuel type and quality, and fuel load), with the only difference being the use of the ESP. The similarity of testing conditions between groups is reflected in the comparable distributions and nearly equal measures of central tendency (mean and median) of flue gas properties, such as chimney draft (Fig. 2a), temperature (Fig. 2b), and most gaseous concentrations (Fig. 2l–o) between the control and treatment groups. These parameters were not significantly different between the control and treatment groups ($p > 0.05$).

In contrast, pronounced differences in PM_1 concentrations between the control and treatment groups ($p < 0.001$) indicate the impact of the ESP on particulate pollutants (Fig. 2c and d). Likewise, BC, EC, and OC, which represent a notable fraction of wood combustion particles, also had significantly different concentrations between the control and treatment groups (Fig. 2e–g). The concentrations of BC, EC, and OC were lower in the treatment group than in the control. The ratio of OC to EC (OC : EC) was higher in the treatment than in the control group, with the difference being significant ($p = 0.026$) at 0.05 level (Fig. 2h). Similarly, AAE, which describes wavelength dependence of absorption behavior of particles was also significantly different between the control and treatment groups (Fig. 2i). Control group AAE values were significantly above 1, plausibly due to organic matter coating in co-emitted BC particles.[41] Treatment-group AAEs were close to 1, although notable outliers occurred at both the upper and lower extremes, suggesting substantial inter-test variability in the ESP effect on

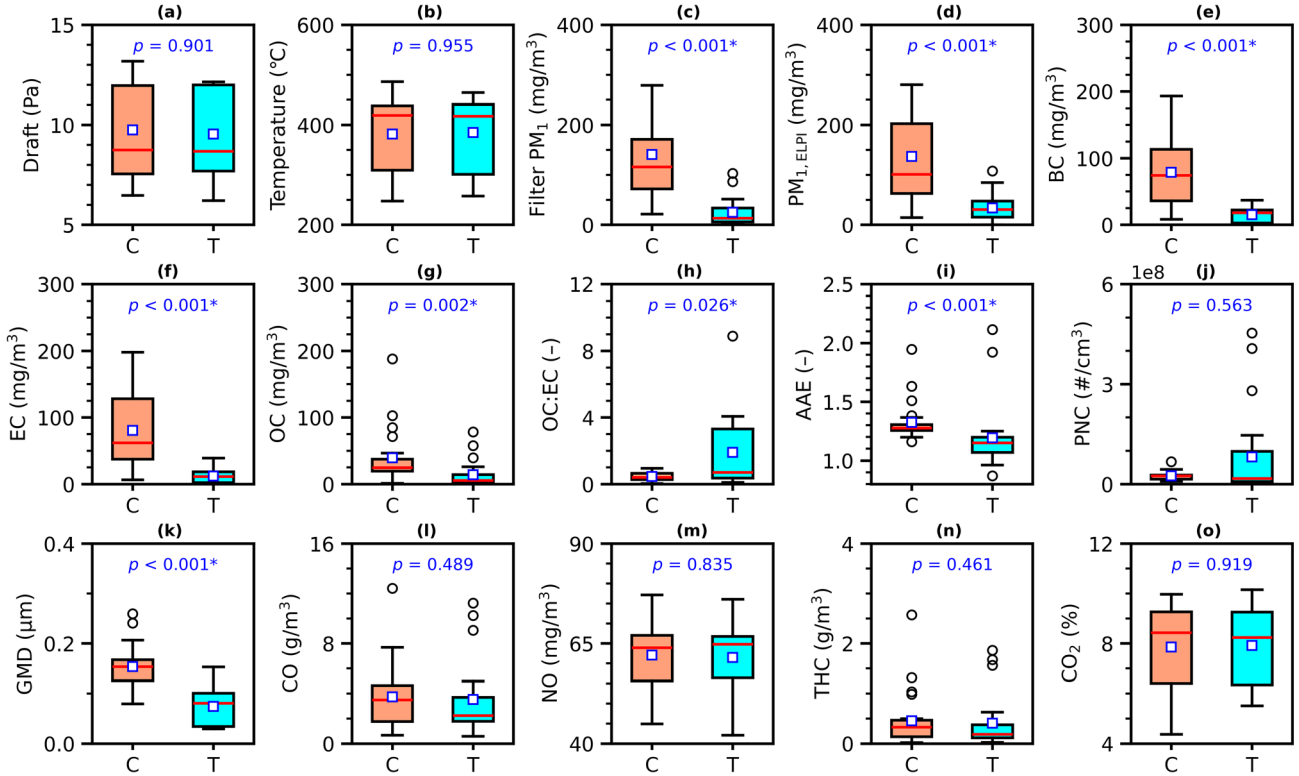

Fig. 2 Comparison of flue gas characteristics between the control (C, $n = 23$) and treatment (T, $n = 22$) groups across all test conditions and stoves. All concentrations are standardized to NTP and 13% O_2. An asterisk (*) with p-value represents a significant difference between the control and treatment groups.

particles. The observed increase in OC : EC ratio in combination with decreased AAE for the treatment group is somewhat surprising and may indicate that the ESP filters brown carbon more efficiently than non-light-absorbing organics. Another possibility could be that the ESP influences the mixing state of OC and EC, and eventually the coating of soot particles, which is known to influence AAE.[43] Overall, these observations suggest that ESPs not only reduce the particle mass concentrations but also significantly alter the chemical composition and optical properties of emitted particles.

Unlike PM_1 concentrations, PNCs in the treatment group were highly right-skewed, with the mean slightly higher than in the control group, whereas the median was lower, indicating a more complex influence of the ESP on PNC (Fig. 2j), which will be discussed in more detail in Section 3.3. Moreover, geometric mean diameter (GMD) in the treatment group was significantly different from that in the control group ($p < 0.001$), suggesting a notable impact of the ESP on particle size distribution (Fig. 2k).

3.2 Effect on particle mass concentration and composition

Mean $PM_{1,ELPI}$ concentration and ESP collection efficiency under different experimental conditions are presented in Fig. 3a. Under the control conditions, mean $PM_{1,ELPI}$ concentrations spanned a wide range of 61.0 mg m^{-3} (MS_BL) to 325 mg m^{-3} (SS_BL, batch 2). Under the treatment conditions, it ranged from 14.0 mg m^{-3} (MS_ESP) to 81.7 mg m^{-3} (SS_ESP, batch 2). The mean gravimetric PM_1 (filter PM_1) ranged from 70.8–223 mg m^{-3} in the control group and 8.4–80.0 mg m^{-3} in the treatment group (SI, Fig. S3). A typical comparison of real-time $PM_{1,ELPI}$ concentrations for SS shows consistently lower concentrations under the ESP treatment than under the control, albeit with a few brief spikes observed in the treatment tests (SI, Fig. S4a and b). In addition, real-time $PM_{1,ELPI}$ concentrations were higher in batch 2 than in batch 1 of SS tests, and the relative reduction achieved with the ESP was lower in batch 2. The batch-average particle mass reduction efficiencies for various control–treatment pairs ranged from 71% (SS_SA *vs.* SS_SA_ESP, batch 2) to 83% (SS_BL *vs.* SS_ESP, batch 1) (Fig. 3a).

Similarly, real-time BC concentrations were also lower under the ESP treatment than under the control throughout the test duration, suggesting an effective collection of soot particles by the ESP (SI, Fig. S4c and d). The batch-average efficiency for BC ranged from 67% (SS_SA *vs.* SS_SA + ESP, batch 2) to 89% (MS_BL *vs.* MS_ESP) (Fig. 3b). For EC, it ranged from 59% (SS_SA *vs.* SS_SA + ESP, batch 2) to 95% (MS_BL *vs.* MS_ESP) (Fig. 3c). The patterns of EC reduction efficiency were similar to those for BC. Moreover, ESP efficiency for OC was relatively low, ranging from 53% (SS_BL *vs.* SS_ESP, batch 2) to 86% (SS_BL *vs.* SS_ESP, batch 1) (Fig. 3d).

For the sauna stove, the ESP efficiencies were higher in batch 1 than in batch 2 for $PM_{1,ELPI}$, EC, and OC (Fig. 3). The mean flue gas temperature was lower in batch 1 (289 ± 21 °C) than in

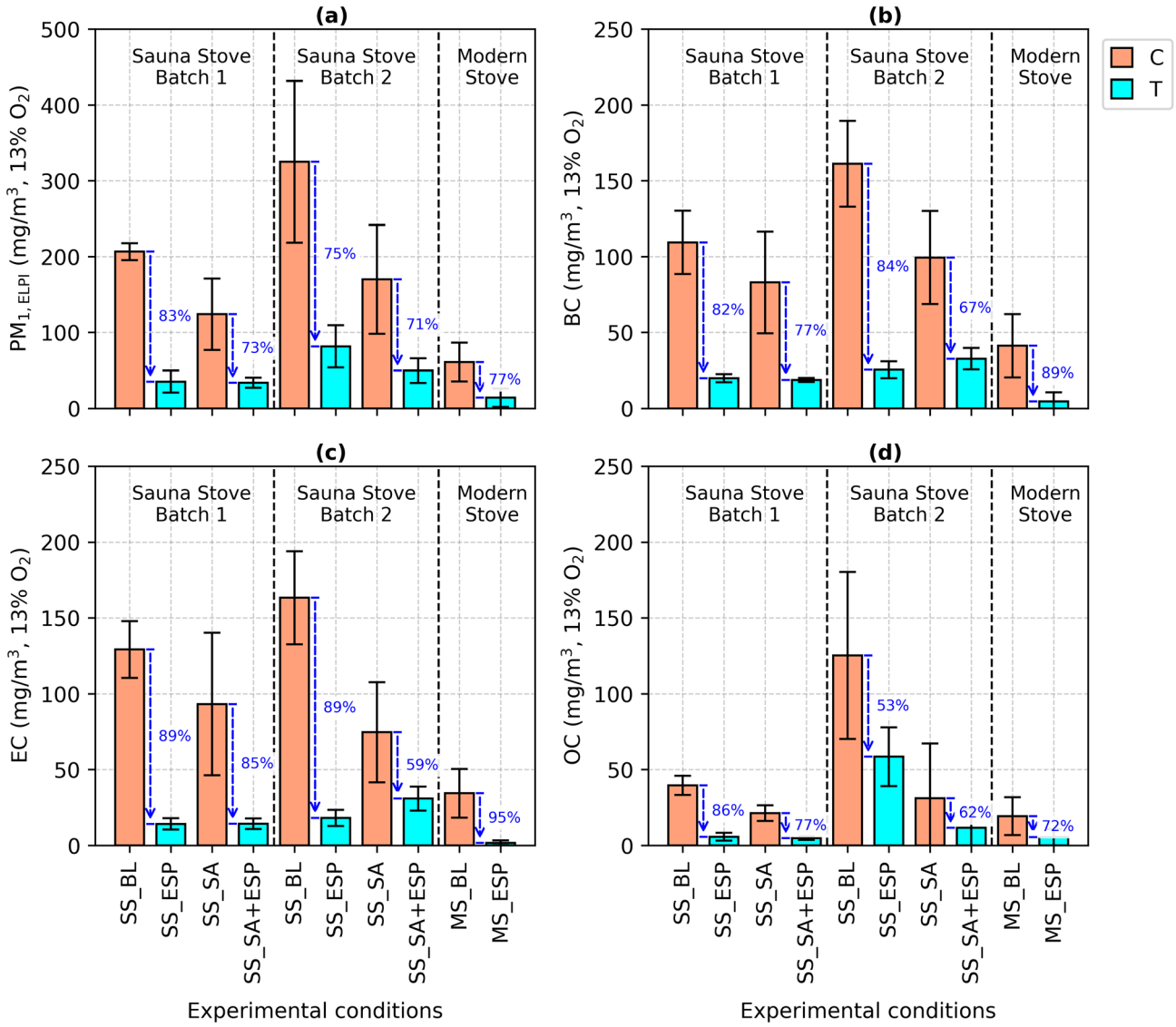

Fig. 3 Comparison of particulate pollutant concentrations between the control and treatment groups under various experimental conditions: (a) $PM_{1,ELPI}$, (b) BC, (c) EC, and (d) OC. To achieve a wide range of emission loads, SS tests were conducted with and without SA supply. All concentrations are standardized to NTP and 13% O_2. Annotated values indicate emissions reduction efficiencies of the ESP. Error bars represent SDs.

batch 2 (454 ± 16 °C). The elevated flue gas temperatures in batch 2 might be a factor responsible for reducing the ESP performance. Although data on ESP operating parameters were not available in this study to directly observe phenomena such as spark-over events, several previous studies reported that elevated temperatures may impair ESP performance.[23,28,29] At temperatures above 300 °C, frequent sparkovers might occur due to the increase in gas conductivity as well as deformation of electrodes, which might interfere with ESP performance.[22] To avoid sparkovers, the working voltage of ESPs should be lowered,[22] which reduces the strength of the electric field and particle charging efficiency.[29] In addition, the flue gas flow rate is higher and the residence time lower at elevated temperatures, which also influences the ESP filtration efficiency. Although newer combustion appliances have high efficiency requirements, meaning that their average flue gas temperatures are low, temperatures can still be occasionally high. Hence, flue gas temperature is of critical importance in ESP design for RWC applications.

The grand mean reduction efficiencies were 75.7% ± 4.7% for $PM_{1,ELPI}$, 79.8% ± 8.2% for BC, 83.2% ± 14.2% for EC, and 70.1% ± 12.6% for OC. The lowest variability was observed for $PM_{1,ELPI}$ collection efficiency (coefficient of variation, CV = 6.2%), whereas the highest variability occurred for OC collection efficiency (CV = 18.0%). Since organic emissions, including OC, are sensitive to combustion conditions, variations in OC collection efficiency may partly reflect differences in those conditions. The particle mass collection efficiencies obtained in the present study are on par with those reported in previous studies.[22,23] However, BC collection efficiency in this study was

higher than previously reported in a similar experiment, which was likely due to lower flue gas temperatures in our experiments.[23] These variations in ESP efficiencies reflect differences in operating conditions and stove types between studies. Collectively, these findings indicate that ESPs are more effective in controlling the BC or EC fractions than OC of RWC particles. When the OC fraction is dominant, a typical condition in inefficient combustion,[9,44] the ESP efficiency for particle mass emission control may be diminished, because a large part of OC is semivolatile that may condense downstream the ESP.

It is worth noting that most particulate pollutant concentrations were higher in batch 2 than in batch 1 during SS operation (Fig. 3). This is mainly because the higher combustion temperature in batch 2 accelerates fuel volatilization, increasing oxygen demand beyond the available supply.[12] The resulting oxygen deficit leads to incomplete combustion, emitting more soot particles and unburnt hydrocarbons. Under such conditions, air staging with primary and secondary air supply can substantially improve combustion in the flame zone and reduce emissions.[9] For example, under the SS_BL condition, the $PM_{1,ELPI}$ concentration in batch 2 was 1.6 times that in batch 1 (increase by 118 mg m^{-3}), whereas under the SS_SA condition the increase was only 1.4-fold (increase by 45.9 mg m^{-3}) (Fig. 3a). This demonstrates the important role of SA supply in controlling wood stove emissions, especially in older-model high-emitting appliances.

To further assess the relative effectiveness of the primary and secondary emission control measures, we compared the reductions in particulate pollutant emissions from the sauna stove achieved by SA supply alone (primary control) and by the ESP alone (secondary control) (Fig. 4). SA supply alone reduced mean $PM_{1,ELPI}$ by 45%, whereas ESP alone reduced it by 78% (Fig. 4a). Similarly, for both BC and EC, the reduction achieved by the ESP was nearly twice that achieved by the SA supply alone (Fig. 4b and c). However, for OC, the SA supply alone had a superior performance in comparison to ESP alone (Fig. 4d). These findings suggest that air staging plays an important role in reducing organic emissions, whereas the ESP predominantly reduces EC. Therefore, combining primary measures, such as air staging, with secondary measures, such as the ESP, could substantially reduce both OC and EC components of the particle mass emissions from RWC appliances.

Sauna stoves are a common RWC appliance in Finland, contributing substantially to emissions, especially of $PM_{2.5}$ and BC. Hence, implementing secondary control using ESPs on sauna stoves could significantly reduce emissions from the RWC sector.[11] Moreover, the Ecodesign Directive (2009/125/EC) sets emission limits for closed-fronted, wood-fueled local space heaters (≤50 kW) at 40 mg m^{-3} at 13% O_2, measured using the heated filter method (EN16510-1:2022 standard).[39] The mean baseline $PM_{1,ELPI}$ concentration in MS (manufactured before the new standard came into effect) was 70.8 mg m^{-3}, which is notably higher than the Ecodesign limit. However, when an ESP was used, the $PM_{1,ELPI}$ concentration decreased to 8.4 mg m^{-3}, thereby complying with the limit. Overall, small-scale ESPs could be a promising secondary control technology, especially for retrofitting older-model or high-emitting RWC appliances to control PM emissions.

We compared OC : EC *vs.* AAE relationships between the control and treatment groups (SI, Fig. S5). In the control group, OC : EC showed a significant positive linear relationship with AAE ($p < 0.001$). The treatment group also showed a weak positive but statistically insignificant relationship ($p = 0.086$). It is worth noting that the treatment group included batches with unusually high OC : EC ratios, likely due to very low particulate matter concentrations downstream of the ESP, which might have increased uncertainty in OC and EC measurements. In both groups, however, AAE values for pure EC (OC : EC ≈ 0) were approximately 1.1 (intercepts of the fitted equations in Fig. S5), consistent with those reported for RWC emissions in a previous study.[45] Moreover, as discussed earlier, the mean AAE decreased, whereas the mean OC : EC ratio increased with ESP compared to conditions without ESP.

We also compared PM_1 composition, specifically the fractions of EC and organic matter (OM), between the control and treatment groups. Although OM : OC ratios vary widely across emission sources and with atmospheric aging, primary organic aerosol from biomass combustion typically ranges from 1.56 to

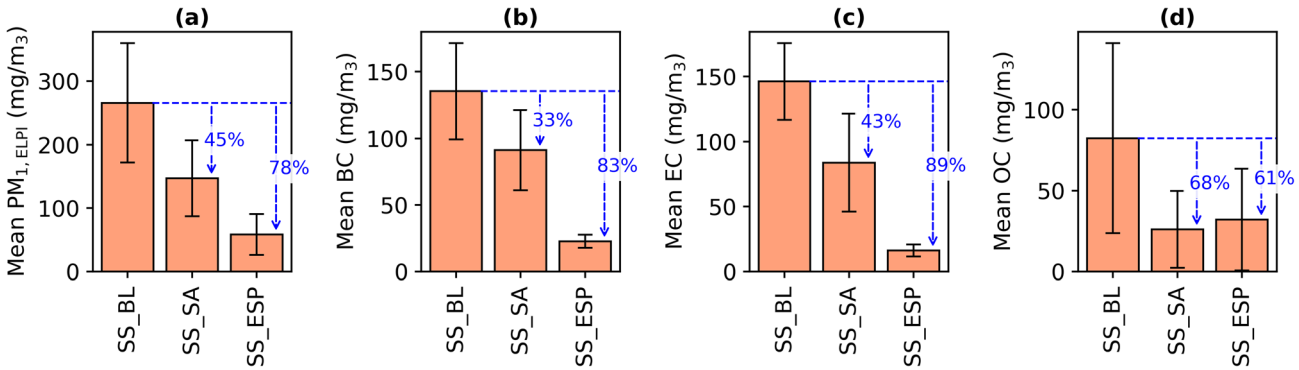

Fig. 4 Comparison of reductions in particulate pollutant emissions achieved by SA supply alone (primary control) and by the ESP alone (secondary control) for the sauna stove: (a) $PM_{1,ELPI}$, (b) BC, (c) EC, and (d) OC. SS_BL denotes the baseline (no SA supply and no ESP), SS_SA denotes the use of SA supply alone (no ESP), and SS_ESP represents the use of ESP alone (no SA supply). Annotated values indicate emissions reduction relative to the baseline. Error bars represent SDs.

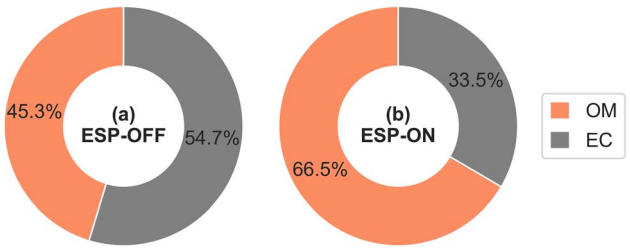

Fig. 5 Relative proportions of OM and EC: (a) control (ESP-OFF) group and (b) treatment (ESP-ON) group.

1.70.[46] We used the upper limit of this range,[46] as it has been adopted in a previous study on RWC emissions.[47] Grand mean OM concentrations, assuming an OM : OC ratio of 1.7, were 66.7 $\pm$ 73.1 mg m^{-3} for the control group and 23.5 $\pm$ 34.8 mg m^{-3} for the treatment group. Corresponding EC concentrations were 80.4 $\pm$ 54.1 mg m^{-3} (control) and 11.8 $\pm$ 11.0 mg m^{-3} (treatment). The relative proportions of OM and EC differed markedly between the control and treatment groups (Fig. 5). The OM fraction increased from 45.3% in the control to 66.5% in the treatment group, whereas the EC fraction decreased from 54.7% to 33.5%. As discussed earlier, the ESP operated with higher removal efficiency for EC than for OM (and OC), resulting in a comparatively higher proportion of OM downstream of the ESP. Another plausible explanation for the enhanced OM fraction is oxidative aging of flue gas within ESPs, potentially facilitated by ozone formed during corona discharge.[37]

3.3 Effect on particle number concentrations and size distribution

Despite consistent effect of ESP on $PM_{1,ELPI}$ concentration, its effect on PNC was heterogeneous across various experimental conditions (Fig. 6). Among the five control–treatment pairs, ESP reduced PNC in three pairs, with the reduction efficiency ranging from 58.6% (SS_BL *vs.* SS_ESP during batch 1) to 73.1% (SS_SA *vs.* SS_SA_ESP during batch 1) (Fig. 6a). In contrast, PNC increased under treatment for the remaining two control–treatment pairs, namely, SS_BL *vs.* SS_ESP (batch 2) and MS_BL *vs.* MS_ESP (Fig. 6a). For these pairs, average PNCs under treatment conditions were 5.3 and 8.0 times those under respective control conditions, indicating a notable increase in PNC with ESP.

For all control–treatment pairs, average particle diameter decreased in the treatment group compared with the control group (Fig. 6b). However, the decrease in particle diameter was very high for SS_BL *vs.* SS_ESP (batch 2) and MS_BL *vs.* MS_ESP (Fig. 6b), which, interestingly, corresponds to the control–treatment pairs that had an increase in PNC under treatment conditions (Fig. 6a). The simultaneous increase in PNC and decrease in GMD suggests possible new particle formation under the treatment condition, consistent with previous observations.[23] This is further supported by comparisons of real-time PNCs. During SS tests, numerous high PNC peaks are observed in the treatment curve during batch 2 combustion (approximately 35–70 min) (SI, Fig. S6). Additionally, the peaks at the beginning of batch 2 correspond to increases in AAE values, suggesting a greater contribution of organic aerosols. Furthermore, real-time PNC and GMD for the MS tests are

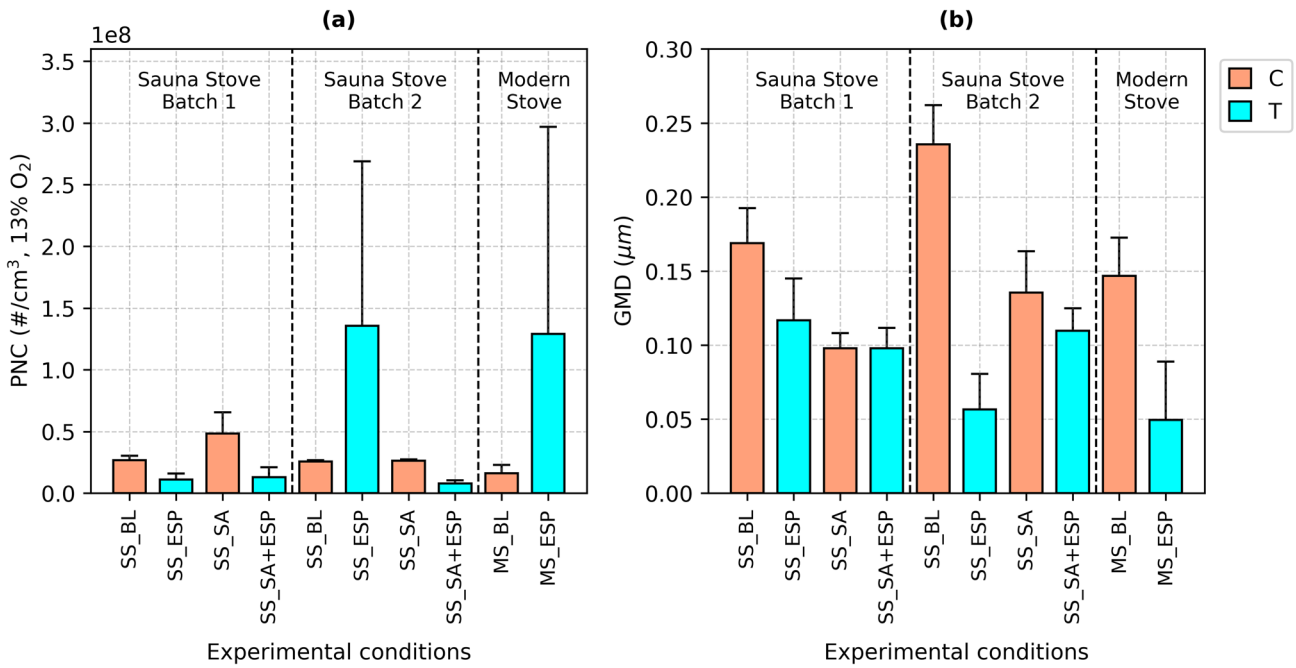

Fig. 6 Comparison of PNC and GMD between the control and treatment groups under various experimental conditions: (a) PNC (standardized to NTP and 13% O_2) measured by CPC and (b) GMD from ELPI. To achieve a wide range of emission loads, SS tests were conducted with and without SA supply. Error bars represent SDs.

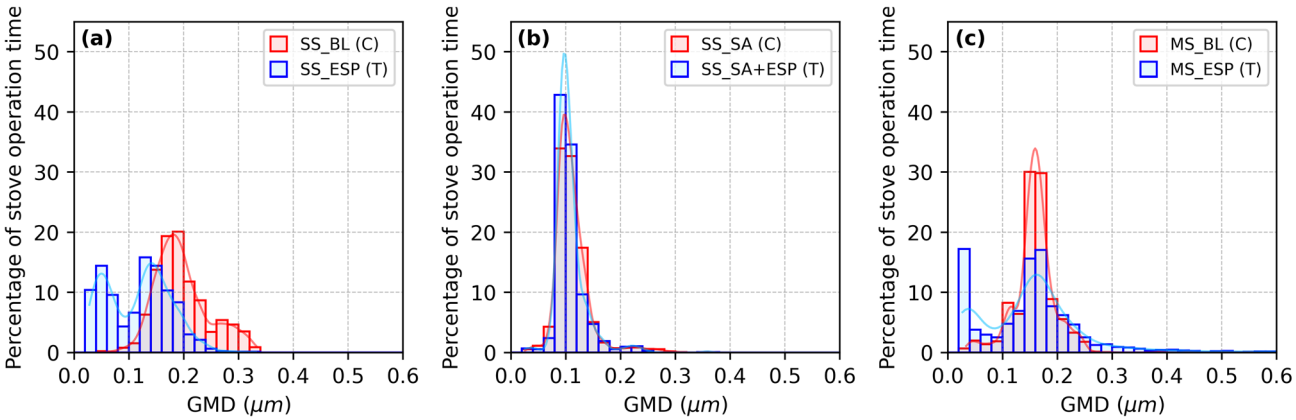

Fig. 7 Histograms of geometric mean diameter of particles under different experimental conditions: (a) SS_BL *vs.* SS_ESP, (b) SS_SA *vs.* SS_SA + ESP, and (c) MS_BL *vs.* MS_ESP.

shown in the SI (Fig. S7). As seen in the figure, PNCs in the control batches remain relatively stable, whereas most treatment batches show substantial fluctuations with distinct peaks that exceed the control levels, particularly at the beginning of the batch. This increase in PNC also corresponds to a decrease in GMD. Although a few PNC peaks also appear in the control batches, they occur only very briefly. In contrast, the PNC peaks in the treatment batches occur more frequently and persist for longer periods.

Particle size behavior with ESP was further evaluated through a frequency distribution of GMD over the entire test period for different control–treatment pairs (Fig. 7). For the SS_BL *vs.* SS_ESP pair (Fig. 7a), the control (SS_BL) exhibits a GMD distribution with a peak at approximately 0.18 μm and another smaller peak at 0.28 μm, whereas the treatment (SS_ESP) shows a clear bimodal distribution with peaks at 0.05 and 0.14 μm. The second peak on the treatment (0.14 μm) is close to the peak on the control (approximately 0.18 μm). However, the first peak on the treatment (0.05 μm), which is absent in the control, plausibly indicates new particle formation. The SS_SA *vs.* SS_SA + ESP pair (Fig. 7b) shows a different behavior, with no clear new peaks observed in the treatment. For the MS_BL *vs.* MS_ESP pair (Fig. 7c), the treatment GMD distribution is again bimodal, with peaks near 0.05 μm and 0.15 μm. Interestingly, the pairs with bimodal distributions correspond to the control–treatment pairs that exhibited negative ESP efficiency for PNC discussed earlier (Fig. 6a). The first peak in the bimodal distributions of treatment groups (Fig. 7a and c) appeared at 0.04–0.05 μm, indicating dominance of nucleation-mode particles for a significant portion of the test duration.

Fig. 8 presents particle number size distribution, as well as the size-resolved effect of ESP on PNC. For the control–treatment pair of SS_BL (batch 2) *vs.* SS_ESP (batch 2), PNC is notably higher for the treatment than for the control below a diameter of 0.12 μm, whereas it is lower for the treatment above 0.12 μm (Fig. 8a). A similar pattern is observed for the MS_BL *vs.* MS_ESP pair, where PNC is higher for the treatment than for the control below a diameter of 0.08 μm. For both cases, the number size distributions in the treatment tests peaks in the nucleation mode. These nucleation-mode particles are unlikely to originate during the combustion process;[48] rather, they were likely formed post-combustion within the ESP. For the remaining cases, PNCs are lower for treatment than for control across the entire size range. Both cases in which the PNC for the treatment exceeds that of the control in at least one of the measured size bins correspond to the negative PNC reduction efficiency of the ESP. In these two cases, the particle number size distributions for the treatments peak at approximately 0.03 μm, with the number size distribution shifted markedly toward nucleation-mode particles.

The PNC reduction efficiency of the ESP as a function of GMD showed an inverted U-shaped trend, with peak efficiency occurring in the 0.1–1 μm size range (Fig. 8b). For particles with diameters >1 μm, the dominant charging mechanism is field charging.[13] However, the field charging efficiency of small-scale ESPs is typically low, which is a likely reason for the significant drop in collection efficiency for particles above 1 μm. Similarly, the lower efficiency for ultrafine particles may be attributed to the formation of new particles. Within the size range of approximately 0.13 to 2.5 μm, the particle number collection efficiency was positive for all control–treatment pairs (Fig. 8b). Because BC typically occurs within this size range, these results indicate that the ESP is most effective at removing soot particles. This is further supported by the significant decrease in the EC fraction observed downstream of the ESP (Fig. 5). The grand mean PNC reduction efficiency (averaged across all control–treatment pairs) peaked at 0.43 μm, reaching 83.5%. Comparable results with efficiency of approximately 80% at the similar size range were observed by Cornette *et al.*,[32] while also submicron particle number collection efficiencies ranging from >90% for a space-charged ESP[27] to as low as 51% to 57% for a tubular ESP[23] have been reported.

Our observations, including changes in PNC, number size distributions, and the chemical properties of aerosols after ESP treatment, strongly, although indirectly, support the possibility of new particle formation within ESPs. Previous studies have proposed several plausible mechanisms that could contribute to new particle formation within ESPs.[15,23,31] ESPs produce

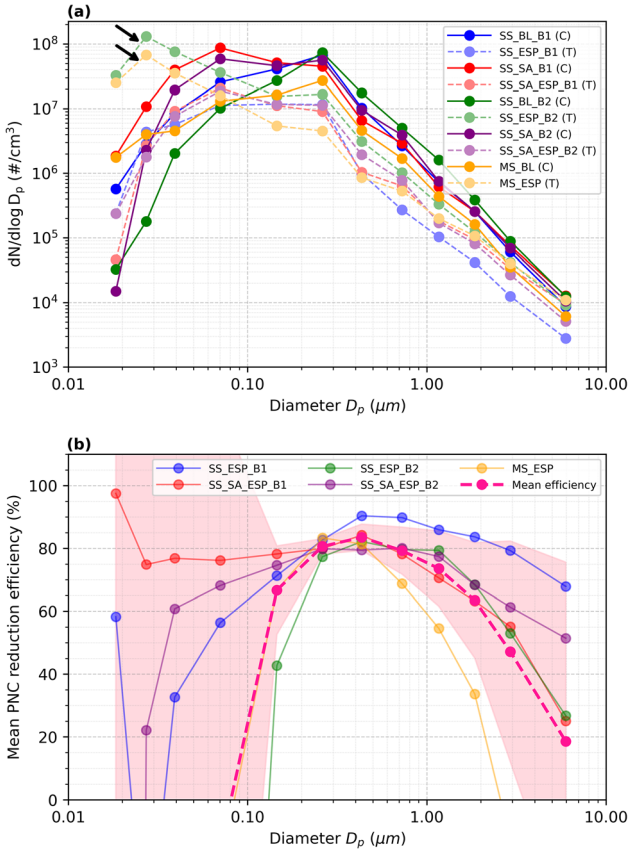

Fig. 8 Size-resolved PNC (standardized to NTP and 13% O_2) and ESP efficiency: (a) particle number and size distributions for the control (C) treatment (T) groups under various experimental conditions; each control–treatment pair is shown in darker and lighter shades of the same color; concentrations are standardized to NTP and 13% O_2; cases of notable increase in nucleation mode particles under the treatment tests are highlighted inside a dotted box, and (b) size-resolved PNC reduction efficiency of the ESP.

ozone due to corona discharge chemistry.[34,35] Free electrons produced in corona discharge may dissociate gas molecules, producing oxygen atoms that may subsequently form ozone.[30] ESP-generated ozone can oxidize organics and potentially contribute to new particle formation. Moreover, ions present in corona discharge environments can generate localized electric fields that attract surrounding molecules, thus promoting nucleation.[30] Possible new particle formation within ESPs has also been observed by Mukherjee *et al.*, who attributed it to the combined effects of the removal of condensation seed particles by ESPs, thus promoting nucleation, and ion- and ozone-mediated oxidation of gaseous organics, both of which promoted the formation of nucleation-mode particles.[23] It is worth mentioning, however, that these mechanisms were not directly observed in the present study. Therefore, these are only plausible explanations, and the evidence for new particle formation is supported only indirectly by our data.

The phenomenon of increased PNC occurred most frequently soon after adding a new wood fuel load to the firebox. It is generally known that, right after fuel addition, the concentrations of organic compounds in the flue gas can be high,[49,50] providing precursors for new particles, which supports this observation. We observed higher upstream OGC concentrations under conditions with negative PNC reduction efficiencies than under conditions with positive PNC reduction efficiencies (SI, Fig. S8a). Furthermore, the upstream OC : EC ratio was higher under the conditions with negative PNC reduction efficiencies (0.57 ± 0.23) than under the conditions with positive PNC reduction efficiencies (0.30 ± 0.17), while the respective AAEs were 1.35 ± 0.21 and 1.28 ± 0.04 (SI, Fig. S8b and c). Higher OGC and OC : EC ratios indicate the dominance of organic emissions. These observations suggest that upstream flue gas composition may affect the PNC reduction efficiency of ESPs and highlight the importance of reducing the organic emissions.

Batch-average OC : EC ratios and GMD showed significant linear relationships, but the nature of this relationship differed between control and treatment groups (SI, Fig. S9). In the control group, GMD increased with increasing OC : EC ratio, plausibly due to organic coating on soot particles,[48] which could lead to larger particle sizes with higher OC loadings (SI, Fig. S9a). In contrast, in the treatment group, GMD decreased as the OC : EC ratio increased (SI, Fig. S9b), which could be due to nucleation of organic vapors, leading to higher OC loadings at smaller sizes.

Overall, our observations indicate a wide variation in the efficacy of ESPs in controlling PNC, depending on RWC appliance operating conditions, emission loads, and chemical composition of particles. The results indicate that, despite their effectiveness in reducing particle mass, ESPs may not adequately control ultrafine PNC in RWC appliances. Hence, regulatory control of ultrafine PNC in RWC emissions remains challenging, as noted in a previous study,[39] and warrants further research.

4 Limitations

Our analysis of emission reduction efficiency of the ESP relied on independent control and treatment measurements rather than simultaneous upstream and downstream measurements, a common approach when simultaneous paired measurements are not feasible. Nevertheless, all known confounding factors, such as fuel quality, fuel load, and refueling frequency, were controlled to minimize inter-test variability, ensuring that observed differences reflect the effect of ESP only.

Despite these efforts, there might still be some unintended variability in combustion conditions. To assess the influence of such unintended inter-batch variabilities in combustion conditions on efficiency estimates, we normalized real-time PM_1 concentrations and PNC by dividing each by the corresponding real-time CO_2 concentrations. These CO_2-normalized values were then used to recalculate the emission reduction efficiencies. A comparison of efficiencies calculated based on actual *versus* CO_2-normalized concentrations is presented in SI (Fig. S10). Ideally, the efficiencies derived from the two methods would be similar. For $PM_{1,ELPI}$, the two methods provided very similar reduction efficiencies. For PNC, however, the efficiencies calculated by the

two approaches were generally comparable, with some noticeable differences in the efficiencies under a few test conditions, especially under the cases of negative PNC reduction efficiencies. In particular, the CO_2-normalized efficiencies showed less extreme values. This suggests that some unintended variabilities in combustion conditions, such as instantaneous combustion rates, might have affected PNC. Nevertheless, key conclusions of the study remain unchanged when CO_2-normalized concentrations are used. Although future studies incorporating simultaneous upstream and downstream measurements of particles as well as quantification of ozone generation, and chemical composition analysis of ultrafine particles could provide further mechanistic insights, our results offer robust evidence of potential new particle formation within ESPs, consistent with recent literature.

5 Conclusions

We analyzed the effect of an ESP on PM_1, EC, OC, number size distribution, and optical properties of particles emitted from two RWC appliances, a sauna stove and a modern stove, both fueled with birch logwood, under conditions spanning a wide range of emission loads. The ESP reduced PM_1 concentrations by 71–83%, EC by 59–95%, and OC by 53–86%, demonstrating high efficiency in particle mass emission control but also indicating substantial variability in performance under different emission conditions and differential collection efficiencies for EC and OC. This variability was partly explained by flue gas temperature, as particle collection efficiencies were lower in combustion batches with higher temperatures in the sauna stove, highlighting the need to consider this factor in ESP design for RWC appliances. Interestingly, we observed an increase in OC : EC ratio in combination with a decrease in AAE of particles with ESP compared to conditions without ESP, which may indicate that ESPs filter brown carbon more efficiently than non-light-absorbing organics. Another possibility could be that the ESP influences the mixing state of OC and EC, and eventually the coating of soot particles, which is known to influence AAE. Overall, our findings suggest that ESPs not only reduce the particle mass concentrations but also significantly alter the chemical composition and optical properties of emitted particles. Furthermore, the ESP consistently reduced PNC in the 0.13–2.5 μm size bin, with the grand mean efficiency peaking at 83.5% at 0.43 μm. In contrast, nucleation-mode PNC increased with ESP in two of five test conditions, suggesting possible new particle formation, which was also supported by a strong shift in size distribution, with an overall decrease in GMD. Our results showed that while ESPs substantially reduce particle mass concentrations, PNC may occasionally increase due to new particle formation. This highlights the challenge of regulating ultrafine PNC in RWC emissions and also warrants the need for further research.

Author contributions

Narayan Babu Dhital: data curation, formal analysis, validation, visualization, writing – original draft; Juho Louhisalmi: methodology, investigation, data curation, Formal analysis, validation, writing – review & editing; Henna Rinta-Kiikka: data curation, validation, writing – review & editing; Sampsa Väätäinen: methodology, investigation, data curation; Jani Leskinen: investigation, writing – review & editing; Olli Sippula: methodology, supervision, validation, writing – review & editing; Jarkko Tissari: conceptualization, methodology, investigation, data curation, formal analysis, validation, funding acquisition, project administration, resources, supervision, writing – review & editing.

Conflicts of interest

Olli Sippula serves as a guest editor for the themed collection "The influence of combustion emissions on air quality and atmospheric processes" in Environmental Science: Atmospheres. The peer-review process was handled by an independent editor. All other authors declare no competing interests.

Data availability

The data supporting this article have been included as part of the supplementary information (SI). Supplementary information is available. See DOI: https://doi.org/10.1039/d5ea00175g.

Acknowledgements

This research was funded by the Finnish consortium project "Kiukaiden ympäristövaikutusten vähentäminen (KIUAS-2)" and the SmokeFreeHomes-Nepal project funded by the Ministry for Foreign Affairs of Finland (Decision 89892623, UH2022-078604) under Develop2 – Development Research Academy Programme.

References

1 F. Wu and S. Pfenninger, Challenges and opportunities for bioenergy in Europe: National deployment, policy support, and possible future roles, *Bioresour. Technol. Rep.*, 2023, **22**, 101430.
2 European Environment Agency, *Share of energy consumption from renewable sources in Europe*, https://www.eea.europa.eu/en/analysis/indicators/share-of-energy-consumption-from, accessed 1 October 2025.
3 C. Sulaiman, A. S. Abdul-Rahim and C. A. Ofozor, Does wood biomass energy use reduce CO_2 emissions in European Union member countries? Evidence from 27 members, *J. Cleaner Prod.*, 2020, **253**, 119996.
4 M. Savolahti, N. Karvosenoja, S. Soimakallio, K. Kupiainen, J. Tissari and V.-V. Paunu, Near-term climate impacts of Finnish residential wood combustion, *Energy Policy*, 2019, **133**, 110837.
5 L. Kangas, J. Kukkonen, M. Kauhaniemi, K. Riikonen, M. Sofiev, A. Kousa, J. V. Niemi and A. Karppinen, The contribution of residential wood combustion to the $PM_{2.5}$ concentrations in the Helsinki metropolitan area, *Atmos. Chem. Phys.*, 2024, **24**, 1489–1507.

6 J. Kukkonen, S. López-Aparicio, D. Segersson, C. Geels, L. Kangas, M. Kauhaniemi, A. Maragkidou, A. Jensen, T. Assmuth, A. Karppinen, M. Sofiev, H. Hellén, K. Riikonen, J. Nikmo, A. Kousa, J. V. Niemi, N. Karvosenoja, G. S. Santos, I. Sundvor, U. Im, J. H. Christensen, O.-K. Nielsen, M. S. Plejdrup, J. K. Nøjgaard, G. Omstedt, C. Andersson, B. Forsberg and J. Brandt, The influence of residential wood combustion on the concentrations of $PM_{2.5}$ in four Nordic cities, *Atmos. Chem. Phys.*, 2020, **20**, 4333–4365.

7 EMEP Centre on Emission Inventories and Projections, *Officially reported emissions data*, https://www.ceip.at/data-viewer-2/overview-dataviewers/officially-reported-emissions-data, accessed 10 November 2025.

8 Statistics Finland, *Energy consumption in households*, https://pxdata.stat.fi/PxWeb/pxweb/en/StatFin/StatFin__asen/statfin_asen_pxt_11zs.px/table/tableViewLayout1/, accessed 1 October 2025.

9 S. Väätäinen, J. Leskinen, H. Lamberg, H. Koponen, M. Kortelainen, O. Sippula and J. Tissari, The effects of air staging and combustion air control on black carbon and other particulate and gaseous emissions from a sauna stove, *Fuel*, 2023, **331**, 125769.

10 M. König, I. Hartmann, F. Varas-Concha, C. Torres-Fuchslocher and F. Hoferecht, Effects of single and combined retrofit devices on the performance of wood stoves, *Renewable Energy*, 2021, **171**, 75–84.

11 M. Savolahti, N. Karvosenoja, J. Tissari, K. Kupiainen, O. Sippula and J. Jokiniemi, Black carbon and fine particle emissions in Finnish residential wood combustion: Emission projections, reduction measures and the impact of combustion practices, *Atmos. Environ.*, 2016, **140**, 495–505.

12 J. Tissari, K. Hytönen, O. Sippula and J. Jokiniemi, The effects of operating conditions on emissions from masonry heaters and sauna stoves, *Biomass Bioenergy*, 2009, **33**, 513–520.

13 W. C. Hinds and Y. Zhu, *Aerosol Technology: Properties, Behavior, and Measurement of Airborne Particles*, Wiley, Hoboken, NJ, 3rd edn, 2022.

14 A. Laitinen and J. Keskinen, Performance of a sonic jet-type charger in high dust load, *J. Electrost.*, 2016, **83**, 1–6.

15 H. Suhonen, A. Laitinen, M. Kortelainen, P. Yli-Pirilä, H. Koponen, P. Tiitta, M. Ihalainen, J. Jokiniemi, M. Suvanto, J. Tissari, N. Kinnunen and O. Sippula, High temperature electrical charger to reduce particulate emissions from small biomass-fired boilers, *Energies*, 2021, **14**, 109.

16 J. H. Turner, P. A. Lawless, T. Yamamoto, D. W. Coy, J. D. McKenna, J. C. Mycock, A. B. Nunn, G. P. Greiner and W. M. Vatavuk, in *EPA Air Pollution Control Cost Manual*, 2002nd edn, 1999.

17 H. Suhonen, A. Laitinen, M. Kortelainen, H. Koponen, N. Kinnunen, M. Suvanto, J. Tissari and O. Sippula, Novel fine particle reduction method for wood stoves based on high-temperature electric collection of naturally charged soot particles, *J. Cleaner Prod.*, 2021, **312**, 127831.

18 T.-Y. Wen, I. Krichtafovitch and A. V. Mamishev, The key energy performance of novel electrostatic precipitators, *J. Build. Eng.*, 2015, **2**, 77–84.

19 A. Bologa, H.-R. Paur, T. Ulbricht and K. Woletz, Particle emissions from small scale wood combustion devices and their control by electrostatic precipitation, *Chem. Eng. Trans.*, 2010, **22**, 119–124.

20 M. Omara, P. K. Hopke, S. Raja and T. M. Holsen, Performance evaluation of a model electrostatic precipitator for an advanced wood combustion system, *Energy Fuels*, 2010, **24**, 6301–6306.

21 T. Lind, J. Hokkinen, J. K. Jokiniemi, S. Saarikoski and R. Hillamo, Electrostatic precipitator collection efficiency and trace element emissions from co-combustion of biomass and recovered fuel in fluidized-bed combustion, *Environ. Sci. Technol.*, 2003, **37**, 2842–2846.

22 T. Brunner, G. Wuercher and I. Obernberger, 2-Year field operation monitoring of electrostatic precipitators for residential wood heating systems, *Biomass Bioenergy*, 2018, **111**, 278–287.

23 A. Mukherjee, A. Hartikainen, J. Joutsensaari, S. Basnet, A. Mesceriakovas, M. Ihalainen, P. Yli-Pirilä, J. Leskinen, M. Somero, J. Louhisalmi, Z. Fang, M. Kalberer, Y. Rudich, J. Tissari, H. Czech, R. Zimmermann and O. Sippula, Black carbon and particle lung-deposited surface area in residential wood combustion emissions: Effects of an electrostatic precipitator and photochemical aging, *Sci. Total Environ.*, 2024, **952**, 175840.

24 E. D. Vicente, M. A. Duarte, L. A. C. Tarelho and C. A. Alves, Efficiency of emission reduction technologies for residential biomass combustion appliances: Electrostatic precipitator and catalyst, *Energies*, 2022, **15**, 4066.

25 Z. He and E. T. M. Dass, Correlation of design parameters with performance for electrostatic precipitator. Part II. Design of experiment based on 3D FEM simulation, *Appl. Math. Model.*, 2018, **57**, 656–669.

26 V. Schmatloch and S. Rauch, Design and characterisation of an electrostatic precipitator for small heating appliances, *J. Electrost.*, 2005, **63**, 85–100.

27 A. Bologa, H.-R. Paur and K. Woletz, Development and study of an electrostatic precipitator for small scale wood combustion, *Int. J. Plasma Environ. Sci. Technol.*, 2011, **5**, 168–173.

28 H. Zhao, Y. He and J. Shen, Effects of temperature on electrostatic precipitators of fine Particles and SO_3, *Aerosol Air Qual. Res.*, 2018, **18**, 2906–2911.

29 N. Wang, L. Ning, J. Fu, Y. Ma, S. Gu, M. Cheng and H. Qi, Impact of temperature on electrostatic precipitator performance with varying electrode configurations, *ACS Omega*, 2025, **10**, 21473–21485.

30 O. Molchanov, K. Krpec and J. Ryšavý, Thermodynamic analysis of multi-pollutant removal in electrostatic precipitation applied to small-scale combustion, *Sep. Purif. Technol.*, 2026, **382**, 135657.

31 O. Molchanov, K. Krpec, J. Horák, L. Kubonová, F. Hopan and J. Ryšavý, Combined control of PM and NO_x emissions

from small-scale combustions by electrostatic precipitation, *Results Eng.*, 2024, **24**, 103255.
32 J. F. P. Cornette, I. V. Dyakov, P. Plissart, S. Bram and J. Blondeau, In-situ evaluation of a commercial electrostatic precipitator integrated in a small-scale wood chip boiler, *J. Electrost.*, 2024, **128**, 103897.
33 A.-L. Schulze, D. Büchner, V. Klix, V. Lenz and M. Kaltschmitt, Biological effects of particulate matter emissions from residential pellet boilers in bacterial assays: influence of an electrostatic precipitation, *Biomass Convers. Biorefin.*, 2019, **9**, 227–239.
34 X. Li, L. Yang, Y. Lei, J. Wang and Y. Lu, A method for removal of CO from exhaust gas using pulsed corona discharge, *J. Air Waste Manage. Assoc.*, 2000, **50**, 1734–1738.
35 M. Pirhadi, A. Mousavi and C. Sioutas, Evaluation of a high flow rate electrostatic precipitator (ESP) as a particulate matter (PM) collector for toxicity studies, *Sci. Total Environ.*, 2020, **739**, 140060.
36 A. Yehia, M. Abdel-Salam and A. Mizuno, On assessment of ozone generation in dc coronas, *J. Phys. D: Appl. Phys.*, 2000, **33**, 831.
37 E. Schneider, H. Czech, A. Hartikainen, H. J. Hansen, N. Gawlitta, M. Ihalainen, P. Yli-Pirilä, M. Somero, M. Kortelainen, J. Louhisalmi, J. Orasche, Z. Fang, Y. Rudich, O. Sippula, C. P. Rüger and R. Zimmermann, Molecular composition of fresh and aged aerosols from residential wood combustion and gasoline car with modern emission mitigation technology, *Environ. Sci.: Processes Impacts*, 2024, **26**, 1295–1309.
38 *SIMO - Residential Wood Combustion Simulator*, https://sites.uef.fi/fine/front-page/simo/, accessed 17 December 2025.
39 J. Louhisalmi, H. Rinta-Kiikka, S. Väätäinen, C. Schön, H. Koponen, O. Sippula, N. B. Dhital, K. Krpec, I. Fraboulet, B. Cea, H. Hartmann and J. Tissari, Particulate matter measurement in residential wood combustion: method comparison and introduction of a novel approach, *Fuel*, 2026, **408**, 137738.
40 M. J. Kleeman, J. J. Schauer and G. R. Cass, Size and Composition Distribution of Fine Particulate Matter Emitted from Wood Burning, Meat Charbroiling, and Cigarettes, *Environ. Sci. Technol.*, 1999, **33**, 3516–3523.
41 J. Tissari, S. Väätäinen, J. Leskinen, M. Savolahti, H. Lamberg, M. Kortelainen, N. Karvosenoja and O. Sippula, Fine particle emissions from sauna stoves: Effects of combustion appliance and fuel, and implications for the Finnish emission inventory, *Atmosphere*, 2019, **10**, 775.
42 J. Tissari, Ph.D. Dissertation, University of Kuopio, 2008.
43 A. Virkkula, Modeled source apportionment of black carbon particles coated with a light-scattering shell, *Atmos. Meas. Tech.*, 2021, **14**, 3707–3719.
44 R. Lindgren, N. García-López, K. Lovén, L. Lundin, J. Pagels and C. Boman, Influence of fuel and technology on particle emissions from biomass cookstoves—Detailed characterization of physical and chemical properties, *ACS Omega*, 2025, **10**, 4458–4472.
45 S. Basnet, A. Hartikainen, A. Virkkula, P. Yli-Pirilä, M. Kortelainen, H. Suhonen, L. Kilpeläinen, M. Ihalainen, S. Väätäinen, J. Louhisalmi, M. Somero, J. Tissari, G. Jakobi, R. Zimmermann, A. Kilpeläinen and O. Sippula, Contribution of brown carbon to light absorption in emissions of European residential biomass combustion appliances, *Atmos. Chem. Phys.*, 2024, **24**, 3197–3215.
46 A. C. Aiken, P. F. DeCarlo, J. H. Kroll, D. R. Worsnop, J. A. Huffman, K. S. Docherty, I. M. Ulbrich, C. Mohr, J. R. Kimmel, D. Sueper, Y. Sun, Q. Zhang, A. Trimborn, M. Northway, P. J. Ziemann, M. R. Canagaratna, T. B. Onasch, M. R. Alfarra, A. S. H. Prevot, J. Dommen, J. Duplissy, A. Metzger, U. Baltensperger and J. L. Jimenez, O/C and OM/OC ratios of primary, secondary, and ambient organic aerosols with high-resolution time-of-flight aerosol mass spectrometry, *Environ. Sci. Technol.*, 2008, **42**, 4478–4485.
47 H. a. C. Denier van der Gon, R. Bergström, C. Fountoukis, C. Johansson, S. N. Pandis, D. Simpson and A. J. H. Visschedijk, Particulate emissions from residential wood combustion in Europe – revised estimates and an evaluation, *Atmos. Chem. Phys.*, 2015, **15**, 6503–6519.
48 J. Tissari, K. Hytönen, J. Lyyränen and J. Jokiniemi, A novel field measurement method for determining fine particle and gas emissions from residential wood combustion, *Atmos. Environ.*, 2007, **41**, 8330–8344.
49 M. Kortelainen, J. Jokiniemi, P. Tiitta, J. Tissari, H. Lamberg, J. Leskinen, J. Grigonyte-Lopez Rodriguez, H. Koponen, S. Antikainen, I. Nuutinen, R. Zimmermann and O. Sippula, Time-resolved chemical composition of small-scale batch combustion emissions from various wood species, *Fuel*, 2018, **233**, 224–236.
50 H. Rinta-Kiikka, K. Dahal, J. Louhisalmi, H. Koponen, O. Sippula, K. Krpec and J. Tissari, The effect of wood species on fine particle and gaseous emissions from a modern wood stove, *Atmosphere*, 2024, **15**, 839.